Local Strain Monitoring of Fiber Reinforced Composites under High Strain Fatigue using Embedded FBG Sensors

Esat S. Kocaman[1], Erdem Akay[2], Cagatay Yilmaz[1], Halit S. Türkmen[2], Ibrahim.B.Misirlioglu[1], Afzal Suleman[3], and Mehmet Yildiz[1*]

[1] Faculty of Engineering and Natural Sciences, Integrated Manufacturing Technologies Research and Application Center, Sabanci University, Orhanli-Tuzla, 34956 Istanbul, Turkey
*meyildiz@sabanciuniv.edu

[2]Istanbul Technical University, Faculty of Aeronautics and Astronautics, Istanbul, Turkey

[3]Department of Mechanical Engineering, Center for Aerospace Research, University of Victoria, Victoria, BC, V8W 3P6 CANADA

Abstract

This work studies the strain monitoring of biaxial glass fiber reinforced epoxy matrix composites under a constant, high strain uniaxial fatigue loading using embedded Fiber Bragg Grating (FBG) optical sensors. Three consecutive FBG sensors written on a same fiber optic cable were embedded within the composite specimen along the gage length to study the distribution and evolution of local strains during the cyclic loading. Results show that local strains measured by FBG sensors under the global constant strain can experience considerable variations as the loading progress demonstrating the effect of local damage on the local strains. Autogeneous heating along the specimens were also monitored using thermocouples mounted on the location of the FBG sensors to investigate the effect of temperature variations on FBG measured strains and damage formation.

Keywords: Polymer-matrix composites, Fatigue, Structural health monitoring, Fiber Bragg Grating.

1. INTRODUCTION

Fiber reinforced composites have outstanding properties such as high specific stiffness and strength among others. They have many applications in various industries ranging from aeronautics, automotive to civil infrastructure. During real life conditions, these materials are exposed to cyclic loads which can cause gradual damage. For the reliable application of composite materials, strain monitoring provides effective means to understand the material behavior during loading. Strain-gages or strain-gage based extensometers are commonly used sensors for strain monitoring. However, they have various drawbacks as they are sensitive to electromagnetic fields and not suitable to be embedded within composite materials. In addition, they have low fatigue resistance which cause unreliable strain monitoring in fatigue.
One of the alternatives to strain gage based sensors for structural health monitoring is Fiber Bragg Grating (FBG) optical sensors. Being small and flexible, FBG sensors can be embedded discretely into composites at locations of interest thereby allowing for the investigation of local strain distribution and evolution without endangering the structural integrity of the host material [1-2]. Contrary to the strain-cased sensors, they are insensitive to the electromagnetic fields and can be readily embedded within composite materials. They also have additional important attributes such as light weight, multiplexing and absolute measurement capability and high corrosion resistance [1-2] which make them ideal for strain and structural health monitoring applications [3-4].

Composite materials experience different damage mechanisms during fatigue unlike metals. Stiffness degradation of fiber reinforced polymer matrix composites in response to cyclic loads is characterized by three distinct stages. Namely, in the first stage comprising the first 15-25 % of fatigue life, the rapid formation and interconnection of matrix cracking causes a sharp, non-linear decrease in stiffness. The second stage accounts between 15-20 % to 90 % of the fatigue life where there is a gradual, and linear decrease in stiffness, which is attributed to crack propagations, fiber debonding and delamination. The final stage is differentiated by a sharp nonlinear decrease in stiffness due to the plurality of fiber breakages [5].

Understanding FBG response under low-cycle fatigue conditions is important in terms of applicability of these sensors to monitor structures that are exposed to repetitive high strain amplitude dynamic loads. To this end, the performance of FBG sensors embedded inside fiber reinforced composites under globally constant high strain cyclic loading is investigated in this study. It is shown that strains from the FBG sensors located at different locations can decrease and significantly deviate from each other as low-cycle fatigue progress, notifying the distinction between the global and local response of the material.

It is well documented in the literature that when a specimen is subjected to cyclic loading, the portion of the mechanical energy is dissipated as heat (also referred to as autogenous heating) causing a rise in the temperature of the specimen [6-8]. In order to investigate a possible correlation between FBG measured local strains and corresponding temperature variations, the autogenous heating of the specimens were also monitored using thermocouples mounted on the specimens for the corresponding locations of the FBG sensors.

2. METHODOLOGY

Resin Transfer Molding (RTM) was used to manufacture the composite specimens. Laboratory scale RTM apparatus with the capability to embed optical fibers into composite parts was used to produce flat panels with dimensions of 620mm x 320mm x 3.5mm. Composite laminates consisted of E-glass fiber and epoxy resin and had a stacking sequence of $[90/0]_{6S}$. Metyx LT300 E10A 0/90 biaxial E-glass stitched fabric was used as the reinforcement with area density of 161 g/m^2 in the 0^o orientation, that is aligned along the resin flow direction in the mold, and 142 g/m^2 in the 90^o orientation, leading to the total area density of 313 g/m^2. The resin is composed of Araldite LY 564 epoxy resin mixed with XB 3403 hardener (manufactured by Huntsman Corporation) with the ratio of 100 and 36 parts by weight. The composite panels were exposed to an initial cure at 65 ^{o}C for 24 hours with a post cure at 80 ^{o}C for 24 hours.

Three 1-mm long FBG sensors with Bragg wavelengths of 1540, 1550 and 1560 nm that are written on the same fiber optic cable with 4 cm intervals were acquired from Technica SA. Prior to manufacturing, the fiber optic cable was fixed onto the 0^o surface of a ply through passing it under fiber stitches. The plies were arranged such that the fiber optic cable was between the 6th and 7th layers of the laminate as shown in Figure 1a. Mechanical test specimens were cut out from the composite panels using a water-cooled diamond circular blade into dimensions of 250 mm × 25 mm × 3.7 mm with a 150 mm gage length.

The length and the loading axis of the specimen were aligned with the 0^o fiber orientation. In specimen with FBG sensors, the middle FBG (1550nm) was positioned at the center of the specimen's gage length and the remaining two sensors were located towards the grips as shown in Figure 1b. All three sensors were oriented along the loading direction. Both ends of

specimens were tabbed with an aluminum tab with a dimension of 50 mm × 25 mm × 1mm using two-component room temperature curing epoxy system (Araldite 2011).

All tests were conducted using an MTS 322 test frame with MTS 647 hydraulic wedge grips using an MTS FlexTest GT digital controller with MTS Station Manager software. Load and displacement data were collected with a built-in load cell (MTS 661.20F-03) and linear variable differential transformer (LVDT), respectively. Strain data was gathered using an axial extensometer (MTS 634.25F-24). The Micron Optics SM230 interrogator with Micron Optics Enlight software was used to collect FBG data. K-type thermocouples were used to measure temperature and corresponding data were collected using a National Instruments NI SCXI-1314 DAQ card in a NI SCXI-1000 chassis with LabVIEW software. All data were acquired at a sampling rate of 100Hz. Temperature data was also used for temperature compensation for the strain monitoring.

3. RESULTS AND DISCUSSION

Figure 1a shows the temperature change for three different thermocouples. The temperature evolution reveals three distinct stages. At the first stage, an initial rise in the temperature is observed followed by a second stage for which the rate of temperature increases smaller than the first stage. Finally, a notable increase prior to final failure occurs at the third stage. Figure 1b shows the variations of maximum strains (i.e., peak strains in the sinusoidal strain form) that are recorded by LVDT and FBG sensors with 4mm apart one another where the middle FBG is positioned at the middle of the specimen gage length.

Noting that the fatigue test on this specimen was conducted under globally constant displacement using the LVDT sensor, it can be expected that FBG sensors provide constant strain values. However, maximum strains gathered from the FBGs were significantly distinct from the global behavior of the specimen. Different sections of the specimens can experience different strain variations during the loading process as inherent heterogeneity of the composite structure causes non-uniform strain distributions and elongations along the specimen gage length.

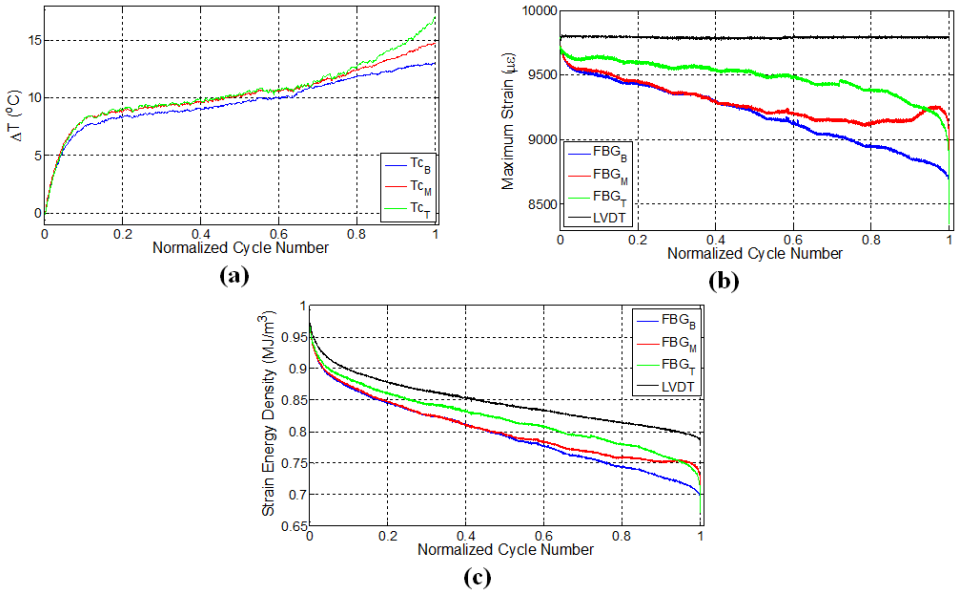

Figure 1: Evolution of temperature (a), strain (b) and mechanical energy (c) for all thermocouples and FBG sensors of specimen 1 where the subscripts B, M, and T denote bottom, midle, and top locations along the gage length of the specimen.

As the fatigue test progresses, the maximum local strains measured by FBG sensors at each cycle decrease such that the trend has three distinct regions: an initial sharp decrease followed by gradual and nearly linear decline and finally sharp drop. Note that these three stages are in agreement with the fatigue phases observed in temperature and strain energy (based on LVDT) plots as a function of cycle number in Figure 1a and Figure 1c, respectively. In addition, strain measured at different locations by the FBG sensors can diverge from each other (i.e. between top and middle FBG sensors). This result indicates the existence of the non-uniform strain distribution due to the local difference in the damage form, density and evolution along the specimen gage length.

A second experiment was conducted using specimen 2 and Figure 2 shows the results. In this test, the cyclic loading was paused after %80 of the fatigue life. The specimen was kept unloaded for 30 min, and then fatigue test was reinitiated while keeping the same test conditions.

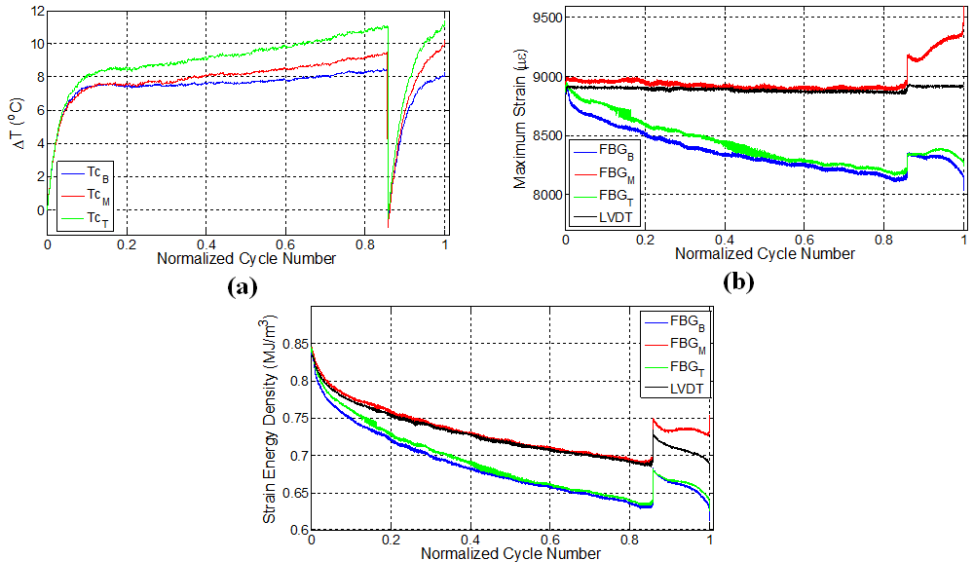

Figure 2: Evolution of temperature (a), strain (b) and mechanical energy (c) for all thermocouples and FBG sensors of specimen 2 where the subscripts B, M, and T denote bottom, middle, and top locations along the gage length of the specimen.

Figure 2a presents variation of surface temperatures at three different thermocouple locations for specimen 2. For the first fatigue loading, similar to previous case (Figure 1a), temperatures of all three locations increase sharply and then follow a gradual linear increase, which corresponds to the second fatigue stage. Upon reinitiating the fatigue loading, it was noted that the rate of temperature rise was higher than that corresponding to the initial fatigue loading. Since the specimen have much higher damage, friction between the newly formed crack or damage surfaces act as sources for heat generation in the specimen, thereby increasing the temperature faster compared to the beginning of the test.

FBG strains and strain energy densities for the specimen 2 are provided in Figures 2b and 2c, respectively. Similar to results of previous experiment, maximum FBG strains decrease throughout the initial fatigue loading. When the fatigue loading was reinitiated, maximum strains measured by FBG sensors experienced sudden jump compared to the maximum strain of the last cycle of the first fatigue loading even though the applied maximum displacement was kept the same. This effect can be attributed to the thermal strain.

As specimen 2 has a higher temperature at the end of the first fatigue loading than at the beginning of the second fatigue loading, portion of the applied strain in the former case is contributed by the thermal strains associated with the thermal expansion of the specimen. When the specimens cool down and the predefined displacement was applied again, contribution from the thermal strain diminishes and more force is needed to induce the desired strain onto the specimen. This results in an upward jump in the measured force and correspondingly the FBG strains.

After the jump in the strain, the maximum strains start to drop down again until %90 of the fatigue life for all of the sensors. The rate of decreases in strain at this stage is significantly different compared to that corresponding to the end of the first fatigue loading for all the respective sensors. At this stage, the strains recorded by top and bottom FBG sensors continue to decrease whereas the strain of the middle FBG starts to increase pointing to significant deformations in the vicinity of the middle FBG sensor.

Both specimen 1 and 2 failed at a location close to the middle FBG. The positions at which the specimens have failed are consistent with the abrupt variations in the strain close to the failure of the specimens as shown in both Figures 1b and 2b. This result indicates that FBG strain was able to provide information for the onset of the specimen failure.

4. CONCLUSION

Fiber reinforced composite specimens with three subsequent FBG sensors embedded along their gage length are exposed to constant, high strain cyclic loads. Considerable differences occurred among the individual FBG sensors and LVDT in the course of the fatigue test demonstrating the distinction between the local and global strain response of the material. This can be attributed to the heterogeneous micro structure of the material causing nonlinear strain distribution and relaxation of the strain in the sensor vicinity due to the formation of various damage mechanisms such as matrix cracking and fiber-matrix debonding. Results indicate that such damage mechanisms observed in fatigue causes FBG strains to follow a trend similar to the stages in stiffness degradation or mechanical energy. In addition, sudden variations in the strains were observed closer to the specimen failure which signals the onset of failure.

Acknowledgments: The authors gratefully acknowledge the funding provided by The Scientific and Technological Research Council of Turkey (TUBITAK), and Ministry of Science, Industry and Technology of Turkey for the project, 112M357, and 01307.STZ.2012-1, respectively.

REFERENCES

[1] A. Cusano, A. Cutolo and J. Albert, Fiber Bragg grating sensors: recent advancements, industrial applications and market exploitation, DOI: 10.2174/97816080508401110101.

[2] Othonos, A. and K. Kalli, Fiber Bragg Gratings, Fundamentals and Applications in Telecommunications and Sensing, 1999. Norwood USA: Artech House Publishing.

[3] Luyckx, G., et al., Strain measurements of composite laminates with embedded fibre Bragg gratings: Criticism and opportunities for research. Sensors, 2010. 11(1): p. 384-408.

[4] C.J.Keulen, E.Akay, F.F.Melemez, E.S.Kocaman, A.Deniz, C.Yilmaz, T.Boz, M. Yildiz , H. S.Turkmen, A.Suleman, Prediction of fatigue response of composite structures by monitoring the strain energy release rate with embedded fiber Bragg gratings, Journal of Intelligent Material Systems and Structures, published online before print December 9, 2014, doi: 10.1177/1045389X14560358.

[5] V. Natarajan, H. Gangarao, Fatigue response of fabric-reinforced polymeric composites, Journal of Composite Materials (2005), 39(17):1541-1559.

[6] Jacobsen, T., B.F. Sørensen, and P. Brøndsted, Measurement of uniform and localized heat dissipation induced by cyclic loading. Experimental mechanics, 1998. 38(4): p. 289-294.

[7] Naderi, M. and M. Khonsari, Thermodynamic analysis of fatigue failure in a composite laminate. Mechanics of Materials, 2012. 46: p. 113-122.

[8] Naderi, M. and M. Khonsari, On the role of damage energy in the fatigue degradation characterization of a composite laminate. Composites Part B: Engineering, 2013. 45(1): p. 528-537.